# Structure and electronic properties of a μ-oxo ruthenium bromide

Matilde Saura-Múzquiz[a,b], Bryce G. Mullens[a], Helen E.A. Brand[c], Brendan J. Kennedy[a,*]

[a] School of Chemistry, The University of Sydney, Sydney, New South Wales, 2006, Australia [b] Department of Materials Physics, Universidad Complutense de Madrid, 28040, Madrid, Spain

[c] Australian Synchrotron, Australian Nuclear Science and Technology Organisation, 800 Blackburn Road, Clayton, Victoria, 3168, Australia

## 1. Introduction

The chemistry and physics of systems containing 4d or 5d elements with partially filled d orbitals are of current interest as a consequence of the delicate interplay between spin-orbit coupling and electron correlations. This often results in unexpected, yet startling, properties such as the proposed spin triplet superconductivity in $Sr_2RuO_4$ [1], the coexistence of ferromagnetism and metallic conductivity in $SrRuO_3$ [2], and the extraordinary high Neel temperature in $SrTcO_3$ [3]. Iridium(IV) oxides with a $d^5$ electron configuration, such as $Na_2IrO_3$ and α-$Li_2IrO_4$, have a $J_{eff}$ ¼ 1/2 ground state that has been intensively investigated in the search for exotic properties [4–6]. Exotic electronic and magnetic properties have been observed in double perovskites including $Ba_3ZnRu_2O_9$ that is a potential quantum spin liquid lacking magnetic order down to 37 mK [7,8]. This is attributed to strong magnetic interactions within the $Ru^5$þ S ¼ 3/2 face-sharing dimers coupled with the geometric, magnetic frustration. A giant magnetoelastic effect is present in the 6H-perovskite $Ba_3BiIr_2O_9$, which contains 5d $Ir^4$þ (S ¼ 1/2) dimerized into isolated face-sharing $Ir_2O_9$ bioctahedra [9].

Recently, attention has expanded from the oxides to include the halides [10]. Of these, α-$RuCl_3$ has arguably garnered the most attention due to its potential to host a Kitaev quantum spin liquid ground state that may be relevant for quantum computing [11,12]. The $A_2BX_6$ halides are alternatively described as antifluorites or vacancy ordered double perovskites. The single-ion behaviour of the hybrid $(CH_3NH_3)_2RuX_6$ (X ¼ Cl or Br) compounds have been explored and the magnetic behaviour of the corresponding alkali metal hexahaloruthenates were recently reported [13,14]. Where the Ru cations are isolated from each other, their magnetic properties are in agreement with the predictions of the Kotani model for low spin $d^4$ systems [15]. Where the cations are not isolated, deviations from the Kotani model are observed [13,14]. Comparison of the structural and magnetic properties of the iridium(IV) halides, $K_2IrCl_6$ and $K_2IrBr_6$, has shown that distortion of the fcc spin lattice in the bromo complex partially alleviates the magnetic frustration observed in the chloro complex [16,17]. Replacing the K cation with Na increase the antiferromagnetic transition temperature from ~2.9 K in $K_2IrCl_6$ to ~7.4 K in $Na_2IrCl_6$. Partial hydration of the sodium ion in $Na_2IrCl_6$ results in distortion of the $IrCl_6$ octahedra impacting the observed magnetic behaviour [18].

Interest in the electronic and magnetic properties of μ-oxo dimers of the 4d and 5d elements intensified with the discovery by Meyer and coworkers that an oxo-bridged dinuclear ruthenium(III) complex $Ru^{III}$–O–$Ru^{III}$ acted as a water oxidation catalyst [19]. Similar activity has been observed in some μ-oxo Ir(IV) dimers [20]. The linear Ru–O–Ru bond in the family of $[Ru_2OCl_{10}]^{4-}$ oxychlorides results in a diamagnetic ground state. The spectroscopic properties of these, and of related osmium, rhenium and tungsten oxychlorides, have been extensively studied. Less is known about the corresponding oxybromides, and the ruthenium compounds in particular are poorly characterised [21]. Indeed, Appleby et al. [22] concluded that the earlier report of the preparation of $Cs_4[Ru_2OBr_{10}]$ by San Filippo and co-workers [23] yielded a heterogenous mixture rather than the desired product. Campbell and Clark described the in situ generation of $[W_2OBr_{10}]^{4-}$ but concluded that this could not be isolated in the solid state [24].

In the present contribution, we provide the first crystallographic study of $K_4[Ru_2OBr_{10}]$ and demonstrate that this is diamagnetic as a consequence of the linear Ru–O–Ru moiety that is seen in the family of $[Ru_2OCl_{10}]^{4-}$ oxychlorides. The Raman and UV–Vis spectra of $K_4[Ru_2OBr_{10}]$ are reported.

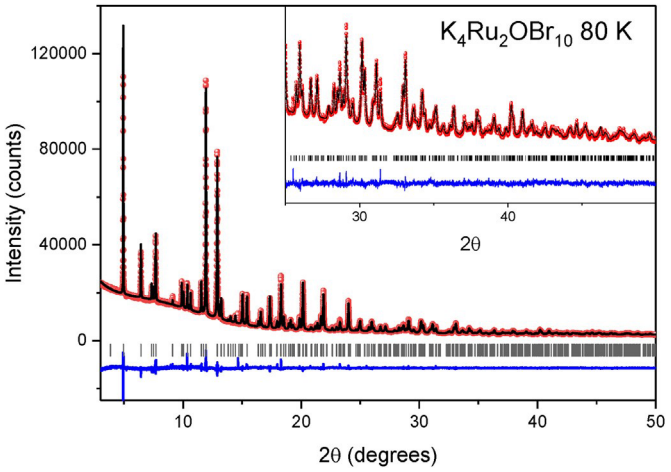


Fig. 1. Rietveld profiles for $K_4Ru_2OBr_{10}$ measured at 80 K with λ¼ 0.5904683 Å. The red symbols are the observed data, the solid black line is the calculated profile, and the lower blue line is the difference between the observed and calculated profiles. The positions of the space group Bragg reflections are indicated by the vertical markers. The inset highlights both the quality of the data and fit to high angle.

## 2. Experimental

The sample was supplied by Surepure Chemicals and used as received. Variable temperature synchrotron X-ray diffraction data were collected from 80 to 300 K on the Powder Diffractometer BL-10 at the Australian Synchrotron using 21.0 keV photons, corresponding to λ ¼ 0.590468 Å based on Rietveld Refinement of $LaB_6$ NIST SRM660B line profile standard. This refinement, using the Thompson Cox Hastings profile function [25], also supplied the instrument resolution function. The sample was placed in a 0.2 mm capillary that was rotated during data collection to minimize preferred orientation effects. The diffractometer uses an array of 16 Mythen II microstrip detector modules. To eliminate the gap between individual modules, two data sets were collected with the detector assembly shifted by 0.5. The resulting data sets were merged using bespoke software [26].

The diffraction pattern was successfully indexed as I-centred tetragonal with a ¼ 7.49541(6) and c ¼ 17.7243(2) Å using the program Conograph [27]. A search of the ICSD database revealed a similar unit cell for $K_4Ru_2OCl_{10}H_2O$ and this was used to create a starting model in space group I4/mmm [28]. The structure, reported by Mathieson et al., contains a water molecule with the oxygen of this located at the 2b site (0 0 ½) [28]. Attempts to refine the atomic displacement parameter (ADP) of this oxygen caused the refinements to diverge and/or return unreasonably large values, suggesting this site was not fully occupied. Refinement of the site occupancy using the Rietveld method as implemented in the program GSAS returned a value within two esds of zero, suggesting the site was effectively empty. Examination of the difference Fourier maps did not reveal any electron density at this site and consequently the water molecule was removed from the model. This structure is equivalent to that reported by Deloume et al. for the anhydrous compound $K_4Ru_2OCl_{10}$ [29]. The background, characteristic of the glass capillary in which the powder sample was packed, was modelled by a twelfth order shifted Chebyshev polynomial. In the final refinement cycles, the profile and lattice parameter were released, and no constraints were placed on the atomic coordinates. The atomic displacement parameters for the oxygen ion refined to physically unreasonable values at the lowest temperatures and so this was set to a small positive value and not refined. All other ADPs were freely refined.

Table 1

Refined structural parameters for $K_4Ru_2OBr_{10}$ at 80 K. The structure was refined in space group I4/mmm with a ¼ 7.49541(6), c ¼ 17.72429(17) Å. Cell volume ¼ 995.772(15) $Å^3$. $R_p$ ¼ 0.0223%, $R_{wp}$ ¼ 0.0297%, $\chi^2$ ¼ 6.22.

| Atom | Site | x | y | z | $U_i/U_e$[b]100 $Å_3$ |
|---|---|---|---|---|---|
| K1 | 4c | 0 | ½ | 0 | 2.35(14) |
| K2 | 4d | 0 | ½ | ¼ | 3.29(15) |
| Ru1 | 4e | 0 | 0 | 0.10243(10) | 2.16(5) |
| O1 | 2a | 0 | 0 | 0 | 2[a] |
| Br1 | 4e | 0 | 0 | 0.24280(14) | 4.31[b] |
| Br2 | 16 m | 0.23763(9) | 0.23763(9) | 0.11161(6) | 2.35[b] |

[a] Value fixed and not varied in the refinements. [b] Anisotropic ADP were refined for the Br anions.

An example of the Rietveld fit is shown in Fig. 1 and the refined atomic coordinates, ADPs and selected bond distances at 80 K are given in Table 1 and Fig. 2.

UV¯Vis¯NIR spectra were measured using a CARY5000 spectrophotometer equipped with a Harrick Omni-Diff probe attachment. All spectral data are reported as the Kubelka¯Munk transform, where F(R) ¼ (1 R)/2R (where R is the diffuse reflectance of the sample relative to the $BaSO_4$ standard) [2].

Raman spectroscopy was undertaken using a Renishaw inVia Reflex Microscope in ambient conditions. A 633 nm HeNe laser was run at 10% intensity to measure 80 <ν < 1000 $cm^1$, with five sets of 30 s acquisitions to improve the signal-to-noise ratio. The statistical occupation of thermal states was accounted for by scaling each intensity by the BoseEinstein occupation factor [30]. XPS were recorded on a ESCALAB250Xi spectrometer using Mg-Kα radiation (1253.6 eV) at 13.8 kV, 8.7 mA with a constant pass energy of 20 eV operating with a vacuum below 2 $10^9$ mbar. Binding energies are referenced to the C 1s signal from adventitious hydrocarbon at 284.8 eV.

The magnetic properties of the powder samples were measured using a DynaCool Quantum Design Physical Property Measurement (PPMS) system equipped with a vibrating sample magnetometer (VSM). The powders were packed into a polycarbonate capsule (VSM Powder Sample Holder P125E) snaped into a brass half-tube sample holder. Zero-fieldcooled (ZFC)/field-cooled (FC) curves were collected in the temperature range of 2.5 K¯300 K using an applied magnetic field of 1000 Oe. Isothermal magnetization data were collected at 2.5 K, scanning the applied field in the range of 9 T.

## 3. Results and discussion

The refined structure of $K_4Ru_2OBr_{10}$ is very similar to that of $K_4Ru_2OCl_{10}$ described by Deloume et al. and consists of discrete binuclear $[Br_5Ru^{-}O^{-}RuBr_5]^{4-}$ anions and Kþ cations. It is isostructural with $K_4Re_2OC1_{10}{\cdot}H_2O$ [31], $K_4Os_2OC1_{10}$ [32], and $K_4W_2OC1_{10}$ [33]. Mattes et al. presented the synthesis of $K_4Ru_2OBr_{10}$ and described this as isostructural with $K_4Ru_2OCl_{10}$, although they provide no further details [21]. Subsequently, Appleby and co-workers failed to isolate the corresponding Cs and Rb salts, concluding that the $A_4Ru_2OBr_{10}$ salts may not exist [22]. The current work unequivocally demonstrates this not to be the case. The two Ru cations in $K_4Ru_2OBr_{10}$ have a distorted octahedral geometry and are linked by the O atom in a linear Ru¯O¯Ru arrangement. The Ru¯O distance, 1.815(2) Å, is comparable to the Ru¯O distance of 1.801(2) Å in $K_4Ru_2OCl_{10}$, and to 1.7838(3) Å and 1.7808(3) Å seen for the two crystallographically unique dimers in the analogous Li compound $Li_4Ru_2OC1_{10}{\cdot}10H_2O$ [34]. The Ru¯Br bond length trans to the bridging O atom is slightly shorter 2.488(3) Å than the four Ru¯Br bonds cis to this, at 2.5242(9) Å. A similar pattern where the axial M-X bond is shorter than the equatorial M-X bond is seen in $K_4Ru_2OCl_{10}$ and $K_4Os_2OCl_{10}$. The four equatorial bromine atoms lie in the same plane and the Ru atom is displaced ~ 0.13 Å out of this plane towards the oxygen atom. The average Ru¯Br distance of 2.512 Å is slightly longer than the

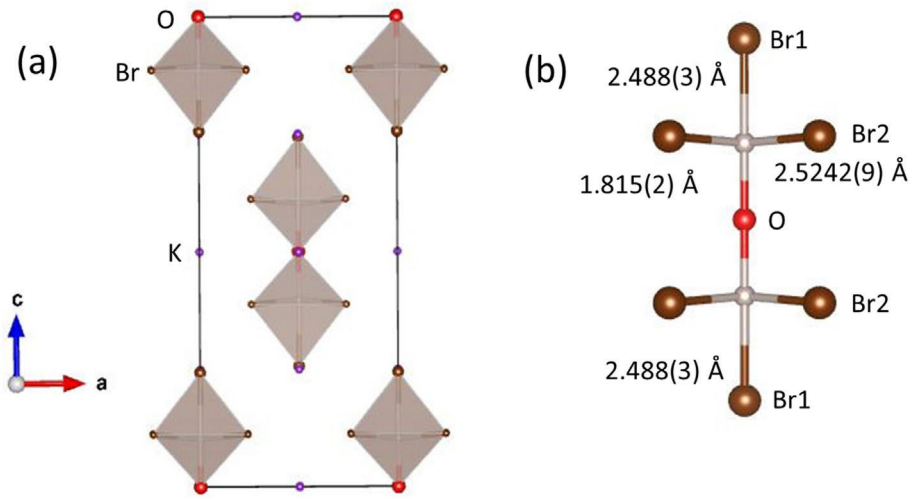


Fig. 2. (a) Representation of the unit cell of $K_4RuOBr_{10}$. The Ru cations are at the centre of the octahedra. (b) Selected bond distances in the $[Ru_2OBr_{10}]^{4-}$ anion. The Br¯Ru¯O¯Ru¯Br linkage is linear. The structure was drawn using VESTA [35].

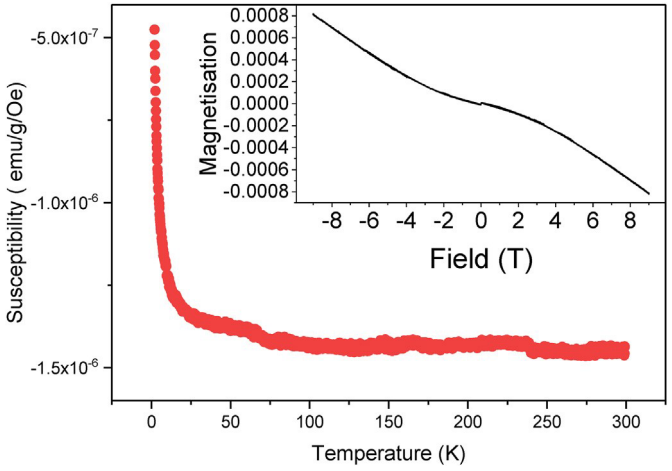


Fig. 3. Variable temperature magnetic susceptibility for $K_4Ru_2OBr_{10}$. The inset shows the magnetization isotherm at 2.5 K.

distance of 2.470(1) Å seen in $K_2RuBr_6$. The structure of $K_4Ru_2OBr_{10}$ is illustrated in Fig. 2.

The two Cs salts, $Cs_4Ru_2OCl_{10}$ and $Cs_4Os_2OCl_{10}$, have orthorhombic symmetry described by space group Pbca [32]. This raises the possibility of a thermally induced phase transition between the tetragonal (I4/mmm) and orthorhombic (Pbca) structures. Variable temperature diffraction studies provided no evidence for such a transition in $K_4Ru_2OBr_{10}$ with the structure remaining tetragonal between 80 and 300 K. Structural refinements against the diffraction data showed that neither the Ru¯O nor Ru¯Br bond distances changed significantly over the studied temperature range. The temperature dependence of the refined bond distances is given in ESI.

Magnetic analysis demonstrated $K_4Ru_2OBr_{10}$ to be diamagnetic under both field cooled (1T) and zero field cooled conditions. This was confirmed by isothermal magnetization measurements that showed negative magnetization behaviour at 2.5 K, Fig. 3. Diamagnetism in the analogous chloro species was initially explained by Dunitz and Orgel by means of a qualitative molecular orbital diagram, that predicted double bond character to the Ru¯O bond [36]. This accounts for the linear arrangement of the Ru¯O¯Ru moiety and the short Ru¯O bond length. Subsequently, Paes and co-workers reported more detailed molecular orbital calculations that extended the simple Dunitz and Orgel model [37]. This work predicts three allowed electronic transitions as observed in the electronic spectra of $[Ru_2OCl_{10}]^{4-}$. The electronic spectra of $K_4Ru_2OBr_{10}$, shown in Fig. 4, displays five features: a weak low-energy peak at 12,600 $cm^{1}$, shoulders at 14,700 and 19,300 $cm^{1}$, and peaks at 22,700 and 31,800 $cm^{1}$. The latter is most likely due to a ligand to metal charge transfer transition. As noted above, the molecular orbital calculations of $[Ru_2OCl_{10}]^{4-}$ predict three allowed transitions. A higher resolution spectrum is necessary to assign the observed features.

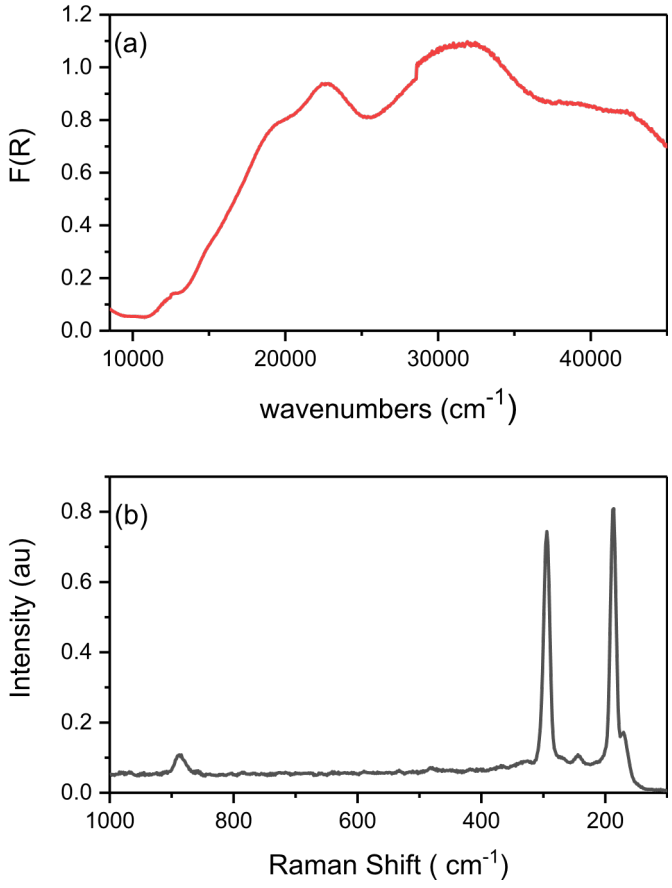


Fig. 4. Solid state (a) UV-VIS-NIR and (b) Raman spectra for $K_4Ru_2OBr_9$. The discontinuity evident near 28,500 $cm^{1}$ in (a) is due to a change in the lamp.

The Raman spectra of $K_4Ru_2OBr_{10}$ displayed five prominent peaks below 1000 $cm^{-1}$ at 168, 186.3, 241, 293.2 and 886 $cm^{-1}$. The peak at 168 and 186.3 $cm^{-1}$ are tentatively ascribed to a Ru-$Br_{ax}$ and Ru-$Br_{eq}$ stretches respectively and that at 241 $cm^{-1}$ to a $\nu_1$ ($A_{1g}$), symmetric metal-oxygen-metal (Ru¯O¯Ru) stretching mode [24]. Polarised Raman measurements would be required to confirm these assignments. The $[RuBr_6]^{2-}$ anion is reported to have peaks at 160, 200 and 302.5 $cm^{-1}$ [38]. X-ray photoelectron spectroscopic measurements showed that the ruthenium to bromine ratio was 1:5.1 consistent with the molecular formula $K_4Ru_2OBr_{10}$. The ruthenium 3d line partially overlaps with the carbon 1s line, see Fig. S2. Curve fitting showed the binding energy Ru $3d_{5/2}$ line to 282.7 eV which falls in the range expected for Ru(IV) compounds.

In summary we report the structure of $K_4Ru_2OBr_{10}$ based on high resolution synchrotron X-ray powder diffraction data. The structural and magnetic properties of this are similar to that described for the isostructural chloride salt $K_4Ru_2OCl_{10}$.

## Author contributions

Matilde Saura-Múzquiz and Brendan J. Kennedy conceived and designed the study. Bryce Mullens carried out the spectroscopic analysis and Helen Brand assisted in the collection of the synchrotron diffraction data. All authors contributed to the data analysis and took part in the writing of the manuscript.

## Declaration of competing interest

The authors declare the following financial interests/personal relationships which may be considered as potential competing interests:

Brendan Kennedy reports financial support was provided by Australian Research Council. Bryce Mullens reports financial support was provided by Australian Institute of Nuclear Science and Engineering.

## Acknowledgements

BJK acknowledges the support of the Australian Research Council for this work that was facilitated by access to Sydney Analytical, a core research facility at the University of Sydney and we thank Dr Michelle Woods for assistance with the Raman measurements. BGM thanks the Australian Institute for Nuclear Science and Engineering for a PGRA scholarship. Part of this work was undertaken at the powder diffraction beamline at the Australian Synchrotron.

## Appendix A. Supplementary data

Supplementary data to this article can be found online at https://doi.org/10.1016/j.jssc.2022.123151.

## References

[1] Y. Maeno, H. Hashimoto, K. Yoshida, S. Nishizaki, T. Fujita, J.G. Bednorz, F. Lichtenberg, Superconductivity in a layered perovskite without copper, Nature 372 (6506) (1994) 532¯534.

[2] Mazin II, D.J. Singh, Electronic structure and magnetism in Ru-based perovskites, Phys. Rev. B 56 (5) (1997) 2556¯2571.

[3] E.E. Rodriguez, F. Poineau, A. Llobet, B.J. Kennedy, M. Avdeev, G.J. Thorogood, M.L. Carter, R. Seshadri, D.J. Singh, A.K. Cheetham, High temperature magnetic ordering in the 4d perovskite $SrTcO_3$, Phys. Rev. Lett. 106 (6) (2011), 067201.

[4] G. Cao, P. Schlottmann, The challenge of spin-orbit-tuned ground states in iridates: a key issues review, Rep. Prog. Phys. 81 (4) (2018), 042502.

[5] Y. Singh, S. Manni, J. Reuther, T. Berlijn, R. Thomale, W. Ku, S. Trebst, P. Gegenwart, Relevance of the heisenberg-kitaev model for the honeycomb lattice iridates $A_2IrO_3$, Phys. Rev. Lett. 108 (12) (2012) 127203.

[6] S.C. Williams, R.D. Johnson, F. Freund, S. Choi, A. Jesche, I. Kimchi, S. Manni, A. Bombardi, P. Manuel, P. Gegenwart, R. Coldea, Incommensurate counterrotating magnetic order stabilized by Kitaev interactions in the layered honeycomb alpha$Li_2IrO_3$, Phys. Rev. B 93 (19) (2016) 195158.

[7] I. Terasaki, T. Igarashi, T. Nagai, K. Tanabe, H. Taniguchi, T. Matsushita, N. Wada, A. Takata, T. Kida, M. Hagiwara, K. Kobayashi, H. Sagayama, R. Kumai, H. Nakao, Y. Murakami, Absence of magnetic long range order in $Ba_3ZnRu_2O_9$: a spin-liquid candidate in the S ¼ 3/2 dimer lattice, J. Phys. Soc. Jpn. 86 (3) (2017), 033702.

[8] T.D. Yamamoto, H. Taniguchi, I. Terasaki, Dynamical coupling of dilute magnetic impurities with quantum spin liquid state in the S ¼ 3/2 dimer compound $Ba_3ZnRu_2O_9$, J. Phys. Condens. Matter 30 (35) (2018) 355801.

[9] W. Miiller, M. Avdeev, Q.D. Zhou, B.J. Kennedy, N. Sharma, R. Kutteh, G.J. Kearley, S. Schmid, K.S. Knight, P.E.R. Blanchard, C.D. Ling, Giant magnetoelastic effect at the opening of a spin-gap in $Ba_3BiIr_2O_9$, J. Am. Chem. Soc. 134 (6) (2012) 3265¯3270.

[10] M. Rossi, M. Retegan, C. Giacobbe, R. Fumagalli, A. Efimenko, T. Kulka, K. Wohlfeld, A.I. Gubanov, M.M. Sala, Possibility to realize spin-orbit-induced correlated physics in iridium fluorides, Phys. Rev. B 95 (23) (2017) 235161.

[11] A. Banerjee, C.A. Bridges, J.Q. Yan, A.A. Aczel, L. Li, M.B. Stone, G.E. Granroth, M.D. Lumsden, Y. Yiu, J. Knolle, S. Bhattacharjee, D.L. Kovrizhin, R. Moessner, D.A. Tennant, D.G. Mandrus, S.E. Nagler, Proximate Kitaev quantum spin liquid behaviour in a honeycomb magnet, Nat. Mater. 15 (7) (2016) 733.

[12] K.W. Plumb, J.P. Clancy, L.J. Sandilands, V.V. Shankar, Y.F. Hu, K.S. Burch, H.Y. Kee, Y.J. Kim, alpha-$RuCl_3$: a spin-orbit assisted Mott insulator on a honeycomb lattice, Phys. Rev. B 90 (4) (2014), 041112.

[13] P. Vishnoi, J.L. Zuo, J.A. Cooley, L. Kautzsch, A. Gomez-Torres, J. Murillo, S. Fortier, S.D. Wilson, R. Seshadri, A.K. Cheetham, Chemical control of spin-orbit coupling and charge transfer in vacancy-ordered ruthenium(IV) halide perovskites, Angew. Chem. Int. Ed. 60 (10) (2021) 5184¯5188.

[14] P. Vishnoi, J.L. Zuo, T.A. Strom, G. Wu, S.D. Wilson, R. Seshadri, A.K. Cheetham, Structural diversity and magnetic properties of hybrid ruthenium halide perovskites and related compounds, Angew. Chem. Int. Ed. 59 (23) (2020) 8974¯8981.

[15] H.C. Lu, J.R. Chamorro, C. Wan, T.M. McQueen, Universal single-ion physics in spin-orbit-coupled $d^5$ and $d^4$ ions, Inorg. Chem. 57 (22) (2018) 14443¯14449.

[16] N. Khan, D. Prishchenko, Y. Skourski, V.G. Mazurenko, A.A. Tsirlin, Cubic symmetry and magnetic frustration on the fcc spin lattice in $K_2IrCl_6$, Phys. Rev. B 99 (14) (2019) 144425.

[17] N. Khan, D. Prishchenko, M.H. Upton, V.G. Mazurenko, A.A. Tsirlin, Towards cubic symmetry for $Ir^4$þ: structure and magnetism of the antifluorite $K_2IrBr_6$, Phys. Rev. B 103 (12) (2021) 125158.

[18] S.S. Bao, D. Wang, X.D. Huang, M. Etter, Z.S. Cai, X.G. Wan, R.E. Dinnebier, L.M. Zheng, $Na_2IrCl_6$: spin-orbital-induced semiconductor showing hydrationdependent structural and magnetic variations, Inorg. Chem. 57 (21) (2018) 13252¯13258.

[19] S.W. Gersten, G.J. Samuels, T.J. Meyer, Catalytic oxidation of water by an oxobridged ruthenium dimer, J. Am. Chem. Soc. 104 (14) (1982) 4029¯4030.

[20] S.B. Sinha, D.Y. Shopov, L.S. Sharninghausen, C.J. Stein, B.Q. Mercado, D. Balcells, T.B. Pedersen, M. Reiher, G.W. Brudvig, R.H. Crabtree, Redox activity of oxobridged iridium dimers in an N,O-donor environment: characterization of remarkably stable Ir(IV,V) complexes, J. Am. Chem. Soc. 139 (28) (2017) 9672¯9683.

[21] R. Mattes, M. Moumen, I. Pernoll, Vibrational-spectra of μ-oxo and μ-nitrido complexes of ruthenium and rhenium, Zeitschrift Fur Naturforschung Section Zeitschrift Fur Naturforschung Section B-a J. Chem. Sci. B 30 (3-4) (1975) 210¯214.

[22] D. Appleby, R.I. Crisp, P.B. Hitchcock, C.L. Hussey, T.A. Ryan, J.R. Sanders, K.R. Seddon, J.E. Turp, J.A. Zora, Upon the electronic structure of the μ-oxo-bis [pentachlororuthenate(IV)] anion and the non-existence of caesium μ-oxo-bis [pentabromoruthenate(IV)], J. Chem. Soc., Chem. Commun. (6) (1986) 483¯485.

[23] J. San Filippo, R.L. Grayson, H.J. Sniadoch, Vibrational spectra of μ-oxo-bridged complexes, Inorg. Chem. 15 (2) (1976) 269¯274.

[24] J.R. Campbell, R.J.H. Clark, Resonance Raman, infrared and electronic spectral studies of the μ-oxo-decahalogenodimetallate species $Ru_2OCl^4_{1^-0}$, $Re_2OCl^3_{1^-0}$, $Os_2OCl^4_{1^-0}$, $Re_2OCl^4_{1^-0}$, $W_2OCl^3_{1^-0}$ and $W_2OBr^4_{1^-0}$, J. Chem. Soc. Faraday Trans. II 76 (1980) 1103¯1118.

[25] P. Thompson, D.E. Cox, J.B. Hastings, Rietveld refinement of Debye-Scherrer synchrotron X-ray data from $Al_2O_3$, J. Appl. Crystallogr. 20 (2) (1987) 79¯83.

[26] K.S. Wallwork, B.J. Kennedy, D. Wang, in: The High Resolution Powder Diffraction Beamline for the Australian Synchrotron, 9th International Conference on Synchrotron Radiation Instrumentation (SRI 2006), Daegu, South Korea, May 28Jun 02, Daegu, South Korea, 2006, p. 879.

[27] R. Oishi-Tomiyasu, Robust powder auto-indexing using many peaks, J. Appl. Crystallogr. 47 (2014) 593¯598.

[28] A. McL Mathieson, D.P. Mellor, N.C. Stephenson, The crystal structure of potassium hydroxychlororuthenate, $K_4Ru_2Cl_{10}O.H_2O$ 5 (2) (1952) 185¯186.

[29] J.P. Deloume, R. Faure, G. Thomasdavid, New determination of crystal-structure of potassium μ-oxo-bis(pentachlororuthenate(IV) and structural refinement of potassium hexachlororuthenate, Acta Crystallogr. Sect. B Struct. Sci. Crystal Eng.

Mater. 35 (MAR) (1979) 558¯561.

[30] A.-M. Welsch, J.L. Knipping, H. Behrens, Fe-oxidation state in alkali-trisilicate glasses - a Raman spectroscopic study, J. Non-Cryst. Solids 471 (2017) 28¯38.

[31] J. Morrow, The crystal structure of $K_4Re_2OCl_{10}.H_2O$, Acta Crystallogr. 15 (9) (1962) 851¯855.

[32] K.-F. Tebbe, H.G. Von Schnering, Die Kristallstruktur des Tetrac€asium-μ-oxodecachlorodiosmat(IV), $Cs_4[Os_2OCl_{10}]$ 396 (1) (1973) 66¯80.

[33] T. Glowiak, M. Sabat, B. Jezowska-Trzebiatowska, Potassium μ-oxodecachloroditungstate(IV), Acta Crystallogr. B 31 (6) (1975) 1783¯1784.

[34] R.S.D. Mudiyanselage, M. Marshall, T. Kong, W. Xie, $Li_4Ru_2OCl_{10}.10H_2O$: crystal structure, magnetic properties and bonding interactions in ruthenium-oxo complexes, Acta Crystallogr. B 76 (5) (2020) 884¯891.

[35] K. Momma, F. Izumi, VESTA 3 for three-dimensional visualization of crystal, and morphology data, J. Appl. Crystallogr. 44 (2011) 1272¯1276.

[36] J.D. Dunitz, L.E. Orgel, 528. Application of molecular-orbital theory to some binuclear co-ordination compounds, J. Chem. Soc. (1953) 2594¯2596, 0.

[37] L.W. Paes, R.B. Faria, J.O. Machuca-Herrera, S.d.P. Machado, The linear μ-oxo-bis volumetric [pentachlororuthenate(IV)] anion. Molecular orbital calculations, Inorg. Chim. Acta. 321 (1) (2001) 22¯26.

[38] R.J.H. Clark, T.J. Dines, Resonance Raman spectroscopy of $[RuCl_6]^{2-}$ and $[RuBr_6]^{2-}$, Mol. Phys. 52 (4) (1984) 859¯870.